# Investigation of $CO_2$ electrolysis on tin foil by electrochemical impedance spectroscopy

*Fabian Bienen*[*†‡], *Dennis Kopljar*[†], *Simon Geiger*[†], *Norbert Wagner*[†] *and Kaspar Andreas Friedrich*[*†‡]

†Institute of Engineering Thermodynamics, German Aerospace Center, Pfaffenwaldring 38-40, 70569 Stuttgart, Germany

‡Institute of Building Energetics, Thermal Engineering and Energy Storage, University of Stuttgart, Pfaffenwaldring 31, 70569 Stuttgart, Germany

**Corresponding Authors**

*Fabian Bienen, E-mail: Fabian.Bienen@dlr.de

*Kaspar Andreas Friedrich, E-mail: Andreas.Friedrich@dlr.de

**KEYWORDS**

$CO_2$ electrolysis, $CO_2$RR, Electrochemical Impedance Spectroscopy, tin, formate, Carbon dioxide, $CO_2$

## ABSTRACT

The conversion of $CO_2$ on tin catalysts via electrolysis leads to valuable chemicals – like CO and formate- and can help to close the carbon cycle. In the current literature catalysts for electrochemical $CO_2$ reduction reaction ($CO_2$RR) are amongst other methods characterized via electrochemical impedance spectroscopy (EIS) in terms of charge transfer resistances neglecting the parallel occurring hydrogen evolution reaction (HER). This may lead to an inapt assignment of the catalyst properties to the $CO_2$RR whereas the impedance spectrum displays features of the parasitic HER or mixed information of both reactions. This circumstance is tackled systematically within this work by analyzing linear-sweep voltammograms and impedance spectra under various experimental conditions in order to get more insights into the processes displayed in the respective impedance spectra. The main finding is that the observed high frequency process displays a charge transfer reaction which contains contributions of the HER and $CO_2$RR and is not appropriate to evaluate catalysts for the $CO_2$RR. This ambiguity was observed for experimental conditions where HER or $CO_2$RR prevailed. Additionally, equivalent circuit model simulations confirmed the occurrence of just one arc in the EIS spectrum for parallel occurring charge transfer reactions on the same electrode.

## Introduction

In order to achieve reduction of $CO_2$ emissions on the order of what is necessary to comply with the goals defined in the Paris agreement, all countries and sectors have to substantially increase their efforts. Beyond other measures, particularly for the carbon-footprint of the industry it is mandatory to develop technologies that can substitute processes that are based on fossil feedstock and which emit $CO_2$ and other green-house gases as a consequence. [1, 2] In that respect,

the electrochemical conversion of $CO_2$ off-gas from industrial plants, bio refineries or, in the long-term, even from the atmosphere to useful chemicals using renewable energy can help to change the role of $CO_2$ from harmful waste to a valuable feedstock for the production of a variety of carbon-based chemicals which are nowadays mainly derived from fossil resources. [1-4] The electrochemical $CO_2$RR can lead to several reaction products such as CO, formate / formic acid, methane, ethylene or methanol. At the same time, the most important parasitic reaction in aqueous electrolytes is the HER.[5, 6] The significance of the HER and the distribution between the $CO_2$RR products highly depends on the catalyst, electrolyte, reactions conditions and electrode potential.[7, 8] In this work we focus on the conversion of $CO_2$ on tin foil electrodes to formate which is used in a variety of different applications, e.g. as de-icing agent, drilling fluid or for silage and tanning if subsequently protonated to formic acid.[9, 10] Most of the $CO_2$RR research papers focus on the conversion of $CO_2$ to CO or formate since only two electrons are needed for this conversions making the reaction mechanisms less complex and achieving better performance. [6, 11] Accordingly, it was shown that the electrochemical conversion of $CO_2$ to formic acid and CO are already close to being competitive with the traditional fossil-based production process.[6, 12] However, there is still a lack of knowledge for the conversion of $CO_2$ to formate on tin electrodes especially regarding the reaction mechanism and degradation phenomena.[6, 8] Electrochemical impedance spectroscopy can approach this lack of information with its ability for *operando* quantifying the resistances of the microscopic processes (e.g. charge transfer, mass transport of educts, adsorption of species) displayed in the impedance spectrum.[13] The challenge is to identify the respective processes which are displayed in the impedance spectrum and assigning these features to the correct physical phenomena.

Several authors used EIS as an additional tool among other methods to compare catalysts presented in their papers and substantiate their arguments. However, there is no study focusing on detailed analysis of the impedance spectrum itself to clearly elucidate the different contributions observable in the spectra and assigning them to specific physico-chemical processes.[14] Specifically for Sn-based electrodes, various authors have performed EIS with different appearance of the spectra suggesting a significant influence of the exact composition of the electrocatalyst, reaction conditions and the chemical environment. Choi et al. performed EIS measurements for Sn and Sn – Pb alloys in $CO_2$ saturated 0.5 M aqueous $KHCO_3$ solution. They observed two arcs in the frequency range of 1MHz – 100 mHz. The presented interpretation focused on the high frequency process which was dependent on the alloy composition without further specifying the underlying chemical process.[15] Two arcs were also observed in the impedance spectrum by Lv et al. who conducted EIS measurements in $CO_2$ saturated 0.1 M $KHCO_3$ in the frequency range of 40 kHz – 10 mHz for Sn deposited on Cu foil and Sn. [16] On the other hand Daiyan et al. who analyzed $SnO_2$ based electrodes in $CO_2$ saturated 0.1 M aqueous $KHCO_3$ solution observed only one semi-circle in the –Nyquist plot which was used for the comparison of the investigated catalysts with regard to their reaction kinetics.[17] Comprehensibly all the above mentioned authors did not investigate the origin of the observed processes displayed in the impedance spectrum in detail since their papers focused on the investigation of catalyst materials and EIS was merely employed to compare the kinetics of the reaction on the specific catalyst. Zeng et al. conducted a slightly more detailed investigation on their EIS measurements for Cu and Cu-Sn foams. The electrolyte was $N_2$ or $CO_2$ saturated 0.1 M $KHCO_3$ and the frequency was varied in the range of 10 kHz down to 100 mHz. For both types of foam and purging gas the spectra showed two arcs while one of the arcs was highly dependent on the

applied potential indicating that this arc represents a charge transfer process. An important result is that in contrast to bare Cu foam the Cu-Sn foam exhibits lower charge transfer resistance values in $CO_2$ saturated 0.1 M $KHCO_3$ solution compared to the $N_2$ saturated electrolyte which was then interpreted that the Cu-Sn foam is more active for $CO_2$RR compared to HER.[18]

Since the HER and $CO_2$RR occur in a competing way parallel on the same electrode we want to emphasize how important it is to be sure about which reaction dominates the processes displayed in the impedance spectrum before taking the results of EIS to evaluate catalysts. To the best of our knowledge no elaborated EIS study exists for the $CO_2$RR on tin foil in aqueous $KHCO_3$ solution, or for the $CO_2$RR in general. Therefore a detailed investigation, as described in this contribution, is necessary to get more insights into the processes displayed in the impedance spectrum.

**Experimental Section**

All experiments were performed in a classic three-electrode setup. The working electrode was tin foil (99.998 %, Alfa Aesar, 0.1 mm thickness) with a diameter of 2 cm and a geometrical surface area of $\pi$ $cm^2$. Before assembling the cell the tin foil electrode was immersed for 30 s in 1.0 M $HNO_3$ (Pan Reac AppliChem 1N) to remove surface impurities followed by rinsing with de-ionized water. In all experiments the reversible hydrogen electrode (RHE) was used as reference electrode whereas platinum foil served as counter electrode. If not stated otherwise the temperature of the electrolyte was 303 K. $KHCO_3$ solutions were obtained by mixing solid $KHCO_3$ (≥ 99%, Roth) with pure water (Resistivity > 18 MΩ). For some of the experiments deuterium oxide (99.9 atom% D, Sigma-Aldrich) was used as solvent for $KHCO_3$. Before starting the experiments, the electrolytes were purged *in-situ* at a flow rate of 0.05 slm for at least 1 h with nitrogen (5.0, Linde) or carbon dioxide (4.5, Linde) depending on the desired

experimental parameters. During the tests the bubbling of the desired gas into the electrolyte continued at the above-mentioned flowrate. If mentioned the pH value was measured by using a pH electrode (InLab® Flex-Micro, Mettler Toledo) in combination with an evaluation unit (S7 Seven2GoTM Pro, Mettler Toledo). For all electrochemical tests a ZAHNER-elektrik GmbH & Co. KG Zennium electrochemical workstation and the corresponding evaluation software Thales® was used.

*Electrochemical characterization*

Electrochemical impedance spectra for tin foil were recorded in the range of 10 mHz to 300 kHz in galvanostatic operation mode. The excitation current for every experiment was 5 mA. The benchmark conditions were 303 K, a load of - 4.77 mA $cm^{-2}$ for a measurement in 1 M $KHCO_3$ aqueous solution saturated with $CO_2$. By conducting experiments at - 3.18 mA $cm^{-2}$, - 4.77 mA $cm^{-2}$, - 6.37 mA $cm^{-2}$ and - 7.96 mA $cm^{-2}$ the current dependency of the impedance spectra of tin could be observed. To investigate the thermal behavior of the impedance spectra of tin a temperature series was carried out for 303 K, 313 K, 323 K and 333 K. The effect of different electrolytes was tested by using 0.1 M, 0.2 M, 0.5 M and 1.0 M aqueous $KHCO_3$ solutions. All solutions were purged with $N_2$ or $CO_2$ before starting impedance measurements. To identify processes involving hydrogen containing species deuterium oxide was used as solvent to generate $KHCO_3$ solutions. For all experiments the cell was polarized for 10 minutes at the desired experimental conditions as pre-conditioning procedure before immediately - no current interruption - recording the impedance spectra. At least three consecutive spectra (approx. 7 min relaxation time under load between each run) were recorded for each experimental parameter set whereby the second spectrum was used for evaluation. In contrast to the first spectrum the

second spectrum has reached a steady-state and the observed changes during the following consecutive spectra were marginal. Experiments were repeated for at least one more time to guarantee reproducible results. For an easier comparison the -Nyquist Data were shifted to the same origin by subtracting the ohmic resistance.

Linear-sweep voltammetry (LSV) was performed to compare the activity of tin foil in different electrolytes. The potential was shifted from + 50 mV to – 1300 mV vs. RHE with a sweep-rate of 1 mV $s^{-1}$. The electrolytes were 1.0 M and 0.1 M $KHCO_3$ solution purged with $CO_2$ or $N_2$. For iR compensation an impedance measurement was conducted after recording the LSV to determine the Ohmic resistance.

The Faraday efficiencies (FE) were measured during galvanostatic EIS measurements applying a constant current of - 4.77 mA $cm^{-2}$ at 303 K. The concentration of the gaseous products $H_2$ and CO in the purging gas stream were quantified by a micro gas chromatograph and averaged over time for at least 60 min with a measurement resolution of 5 min. The averaged concentrations were then multiplied with the volume flow of the purging gas stream to obtain the gas flow of the reaction products. By calculating the ratio of the experimental and theoretical product flows (applying faradays law) the FE was determined. The FE for formate was calculated as difference from 100% and the FEs of $H_2$ and CO since tin is known to exclusively produce $H_2$, CO and formate in aqueous alkaline media.[19, 20] Nevertheless, to proof this assumption exemplarily formate was determined to close the mass balance. This was done via UV spectroscopy after converting formate to formic acid and expelling dissolved $CO_2$ and bicarbonate from the liquid sample (interference on detection peak at ca. 220 nm) using $H_2SO_4$ (cf. Figure S1). [21]

## Results and Discussion

Electrochemical impedance spectroscopy is a powerful tool to elucidate rate-determining processes in a specific time domain during electrochemical reactions. However, the analysis of impedance spectra is not trivial and one needs to have detailed knowledge on the contributions that can be observed in the spectra. However, performing a literature survey on this topic it becomes clear that the origins of the processes displayed in impedance spectra obtained for tin foil during $CO_2$ electrolysis are not well understood as – to the best of our knowledge – no detailed analysis has been conducted so far. Combining linear-sweep voltammetry (LSV), faraday efficiency and impedance measurements we want to give insights about the nature of the processes during $CO_2$ reduction on tin foil in $KHCO_3$ aqueous solution.

*Linear-sweep voltammetry and apparent Tafel analysis*

As a starting point to introduce the system that is being studied, LSV measurements were collected in $CO_2$ and $N_2$ saturated 0.1 M and 1.0 M $KHCO_3$ electrolyte with a sweep rate of 1 mV $s^{-1}$ and are depicted in **Figure 1 a)**. For both concentrations, tin foil shows a higher activity in $CO_2$ saturated environment at lower potentials whereas the activity in the high overpotential region is superior in $N_2$ saturated electrolyte. This might be explained due to mass transportation effects of $CO_2$ and a hindrance of the HER reaction at higher current densities. The LSVs were used to perform apparent (not taking partial current densities into account) Tafel analysis which can be seen in **Figure 1 b)**. For each combination of purging gas and electrolyte concentration one can distinguish two regions in the diagram. The increase of the Tafel slopes observed at higher potentials indicate that mass transport effects or other processes contribute to the slope and determine the shape of the plot in this region.[22] The slopes in both $N_2$ saturated electrolytes

and in $CO_2$ saturated 1.0 M $KHCO_3$ in the low potential region are close to -118 mV $dec^{-1}$ which is expected for the HER where the Volmer step is rate limiting.[23] A rate-limiting electron transfer in $CO_2$RR (cf. Eq (5)) would result in a Tafel slope of -118 mV $dec^{-1}$ as well.[24, 25] When analyzing the faraday efficiency for HER (cf. **Figure 1 b)**), which was determined at a constant potential of -550 mV vs. RHE (Region I in Tafel plot), one can see that hydrogen evolution prevails in $CO_2$ saturated 0.1 M and 1.0 M $KHCO_3$ solution at this potential. This fact indicates that the apparent Tafel slope in $CO_2$ saturated electrolyte might be mainly determined by the HER in region I. On the other hand in $CO_2$ saturated 0.1 M $KHCO_3$ solution the Tafel slope is -160 mV $dec^{-1}$ which significantly deviates from -118 mV $dec^{-1}$ expected for HER and a rate limiting electron transfer during $CO_2$RR. This higher Tafel slope indicates a change in the reaction mechanism for the HER (de-activation of active sites induced by $CO_2$) or an increasing contribution of the $CO_2$RR (assuming a mechanism with a Tafel slope greater than 118 mV $dec^{-1}$ for this reaction with uncertain mechanism) to the apparent Tafel slope.

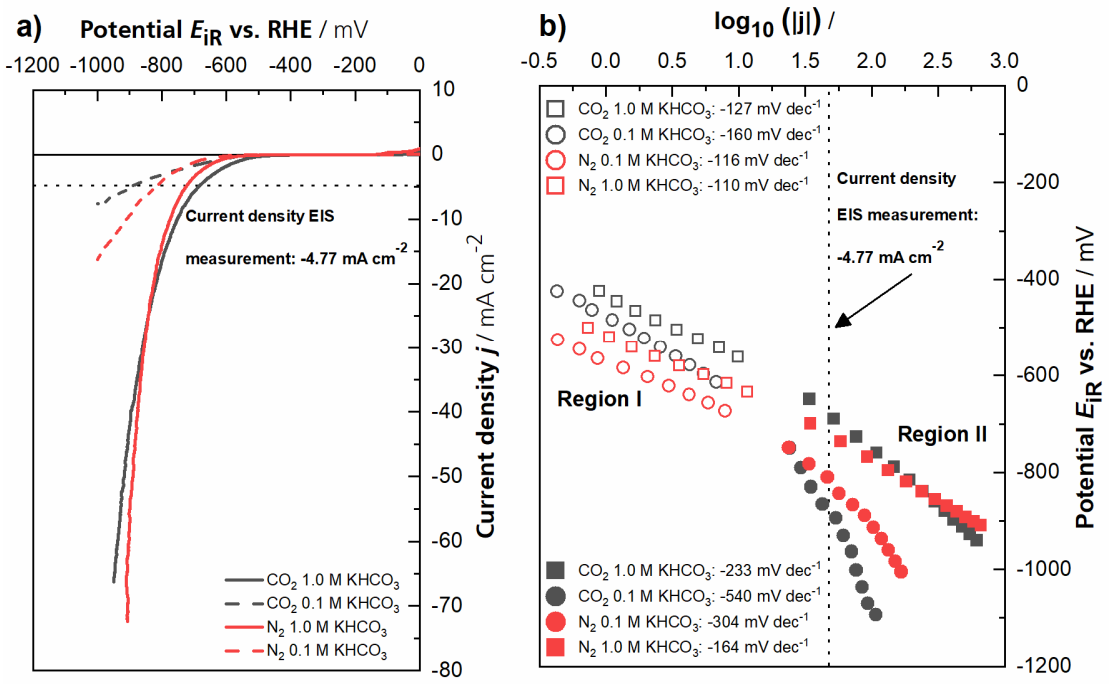


**Figure 1 a)** Linear-sweep voltammetry at 1 mV $s^{-1}$ for tin foil in $N_2$ and $CO_2$ saturated 0.1 M and 1.0 M $KHCO_3$ aqueous solution **b)** corresponding Tafel analysis based on total current ($I_{CO2RR}$ + $I_{HER}$).

*Electrochemical impedance spectroscopy*

FE for $H_2$ and CO were determined during galvanostatic impedance measurements using gas chromatography. The received results and additional information regarding potential and pH values after 1h of bubbling with $N_2$ and $CO_2$, respectively, are shown in **Table 1**.

**Table 1** FE for tin foil in $N_2$ and $CO_2$ saturated 0.1 M and 1.0 M $KHCO_3$ at -4 .77 mA $cm^{-2}$

| Purging Gas | Electrolyte | Potential $E_{iR}$ vs. RHE / mV | FE $H_2$ | FE CO | FE $HCOO^-$ | pH after 1 h Bubbling |
|---|---|---|---|---|---|---|
| $CO_2$ | 1.0 M $KHCO_3$ | -682 | 87% | 3% | 10%* | 8.0 |
| $CO_2$ | 0.1 M $KHCO_3$ | -879 | 43% | 5% | 52%* | 7.1 |
| $N_2$ | 1.0 M $KHCO_3$ | -722 | Only $H_2$ detected | | | 8.9 |
| $N_2$ | 0.1 M $KHCO_3$ | -821 | Only $H_2$ detected | | | 9.2 |

* Calculated using $FE_{H2}$ and $FE_{CO}$ and mass balance closing condition.

As described above impedance measurement were conducted at a current density of -4.77 mA $cm^{-2}$ (15 mA) in galvanostatic operation mode with an excitation signal of 5 mA. After saturating the electrolyte for 1 h with $N_2$ or $CO_2$ the pre-conditioning phase was 10 minutes at the desired experimental parameter set. **Figure 2** shows the –Nyquist and imaginary part vs. frequency plot. In general the spectra reveal at least two processes during electrolysis with a low frequency process occurring at a characteristic frequency around 0.1 Hz and a high frequency process at around 500 Hz. The spectra recorded in $N_2$ saturated electrolytes are dominated by the HER, as no $CO_2$RR products were detected via μ-GC. In general changing the purging gas to $CO_2$ results in bigger diameters for both semi-circles and as a consequence to an increased total faradaic impedance. When bubbling $CO_2$ into the electrolyte additionally to HER the $CO_2$RR must now be taken into account. Accordingly, the increased impedance values might be a result of the

sluggish $CO_2$RR becoming more accented or that the $CO_2$ saturated environment slows down the HER. In order to reveal the origin of the processes we introduce the investigation regarding thermal- and potential activation of the two processes.

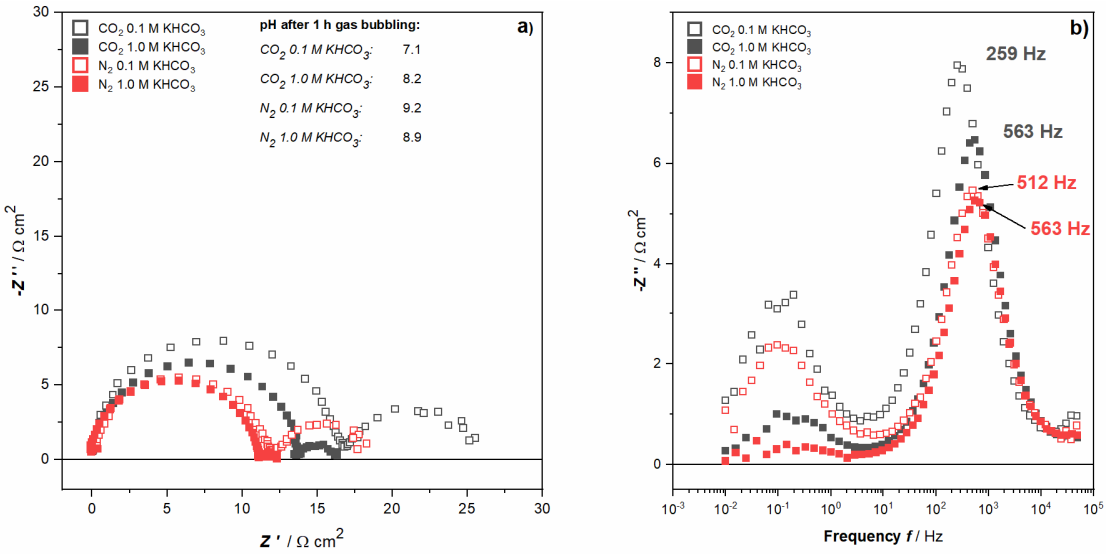


**Figure 2 a)** –Nyquist plot for tin foil obtained in $CO_2$ and $N_2$ saturated 0.1 M and 1.0 M $KHCO_3$ at galvanostatic operation, - 4.77 mA cm-2, with an amplitude of 5 mA, ohmic resistance subtracted **b)** corresponding imaginary part vs. frequency plot.

*Temperature and current dependent behavior*

To identify thermal and current activated processes impedance spectra for the temperature series were recorded at 303 K, 313 K, 323 K and 333 K in $CO_2$ saturated 1.0 M and 0.1 M $KHCO_3$ solution at a current density of - 4.77 mA $cm^{-2}$ while for the current series spectra were recorded at –3.18 mA $cm^{-2}$, –4.77 mA $cm^{-2}$, –6.37 mA $cm^{-2}$ and – 7.96 mA $cm^{-2}$ at 303K (Figure S2 for 1.0 M $KHCO_3$ , Figure S3 for 0.1 M $KHCO_3$).

Taking the obtained results of the current density and temperature variation into account it is very likely that the high frequency process which is activated by increasing temperatures and

current densities displays a charge transfer.[13, 26] Consequently a plot of the $R_{Ct}$ values versus the reciprocal current should result in a straight line whereas the slope represents the Tafel slope (cf. Eq (1) and insets in Figure S2 and Figure S3).[27]

$$R_{Ct} = \mathrm{b} \bullet \frac{1}{2.303 \bullet I} \qquad (1)$$

It is important to mention that the plotted reciprocal current is the total current and not a partial current for HER or $CO_2$RR. The slopes of these plots for 0.1 M and 1.0 M $KHCO_3$ are -163 mV $dec^{-1}$ and -132 mV $dec^{-1}$ which are in agreement with the Tafel slopes obtained via LSV. In consequence the shape of the curve for $CO_2$ saturated electrolytes in Region 1 in **Figure 1 a)** is determined by an electron transfer. The fact that plotting the reciprocal total current vs. $R_{Ct}$ leads to the expected straight line and comparable Tafel slopes to the values found via LSV evaluation suggests that the $R_{Ct}$ arc in the EIS spectrum is a mixed quantity consisting of contributions of the HER and $CO_2$RR. Because of the contribution of both reactions to the Tafel slope in the kinetic region two different explanations exist for an increased Tafel slope in $CO_2$ saturated compared to $N_2$ saturated electrolyte. On the one hand the presence of $CO_2$ could slow down the HER, increasing its magnitude and resulting in an increased mixed Tafel slope whereas on the other hand, the presence of $CO_2$ obviously results in $CO_2$RR taking place at the electrode which might have a significantly higher Tafel slope than the HER and by that pushing the mixed Tafel slope to a higher value.

The low frequency process cannot be attributed to a charge transfer process since it is not activated with increasing temperature and current density in the probed current density range (cf. Figure S2, Figure S3). To gain further insights into the high and low frequency processes

additional experiments with varying $KHCO_3$ concentrations and isotope labeled water were conducted.

*Kinetic Isotope effect*

Impedance spectra were recorded in $CO_2$ saturated 0.1 M and 1.0 M $KHCO_3$ solutions using ultra-pure water or deuterium oxide ($D_2O$) as solvent (303 K, – 4.77 mA $cm^{-2}$). This should give insight into the mechanism of the processes, as slower kinetics of proton involved processes are expected due to the additional neutron in the deuterium core. A simplified reaction mechanism for HER in alkaline media including the Volmer-, Heyrovsky- and Tafel reaction is given in equation (2) – (4) which point out the involvement of hydrogen in the charge transfer reactions (2) and (3).[23]

$$\mathrm{M} + \mathrm{H_2O} + \mathrm{e^-} \rightleftharpoons MH_{ads} + \mathrm{OH^-} \tag{2}$$

$$MH_{ads} + \mathrm{H_2O} + \mathrm{e^-} \rightleftharpoons M + \mathrm{OH^-} + H_2 \tag{3}$$

$$2\,MH_{ads} \rightleftharpoons 2\,M + H_2 \tag{4}$$

Regarding the reaction mechanism of the conversion of $CO_2$ to formate or CO there is no unequivocal and concluding consensus in the scientific community yet. Typically, the first step is considered to be the activation of $CO_2$ through a direct electron transfer followed by a protonation with a simultaneous electron transfer (cf. Eq (5) – (6)).[8, 28] The fact that the $CO_2$ radical formation is often referred to be the rate determining step suggests that a possible displayed charge transfer in the impedance spectrum which is attributed to the $CO_2$RR must then represent a non-concerted proton and electron transfer to $CO_2$.[5, 29]

$$CO_2 + e^- \rightleftharpoons CO_2^{-\cdot} \quad (5)$$

$$CO_2^{-\cdot} + H_2O + e^- \rightleftharpoons HCOO^- + OH^- \quad (6)$$

As a result of the above made considerations we expect, in contrast to the HER, that a $CO_2$RR attributed charge transfer process shown in the spectrum will not be decelerated, resulting in a higher resistance and lower characteristic frequency, when substituting hydrogen with deuterium.[30, 31] We would expect quite the contrary, an acceleration of the $CO_2$RR because the solubility of $CO_2$ increases from 33.8 mmol $L^{-1}$ in $H_2O$ to 38.1 mmol $L^{-1}$ in $D_2O$.[32]

However, the high and low frequency processes are both slowed down when using $D_2O$ as solvent in 1.0 M $KHCO_3$ and in 0.1 M $KHCO_3$ where $CO_2$RR prevails (cf. **Figure 3** and Figure S4 for 1.0M $KHCO_3$). This fact can be seen in larger diameters of the arcs in the high and low frequency region and a reduction of the characteristic frequencies. Since the high frequency process displays a charge transfer reaction affected by $CO_2$ one can now be a bit more specific that this charge transfer process involves hydrogen or a hydrogen containing species. This observation rules out that the observed charge transfer is dominated by the conversion of $CO_2$ to the $CO_2^{\cdot-}$ radical (cf. Eq (5)) leading to the suggestion that this process might be ascribed to the HER. On the other hand, since the mechanism of $CO_2$RR to $HCOO^-$ and CO is not fully understood yet, it might be that (in contrast to Eq (5)) a hydrogen containing species is involved in the rate limiting $CO_2$RR charge transfer reaction. For example, Baruch et al. suggested the involvement of hydrogen containing tin carbonate species in the rate limiting $CO_2$RR charge transfer. Analogous to the involvement of hydrogen during HER the unlikely, but not completely excluded, participation of a bicarbonate species during $CO_2$RR would result in an increase of the

high frequency resistance as well when substituting $H_2O$ with $D_2O$.[33] As it will be shown later the low frequency arc correlates with the $HCO_3^-$ concentration so that a slowed down low frequency process in $D_2O$ based electrolytes might be explained by a impeded movement of $HCO_3^-$ and $DCO3^-$ ions in $D_2O$.

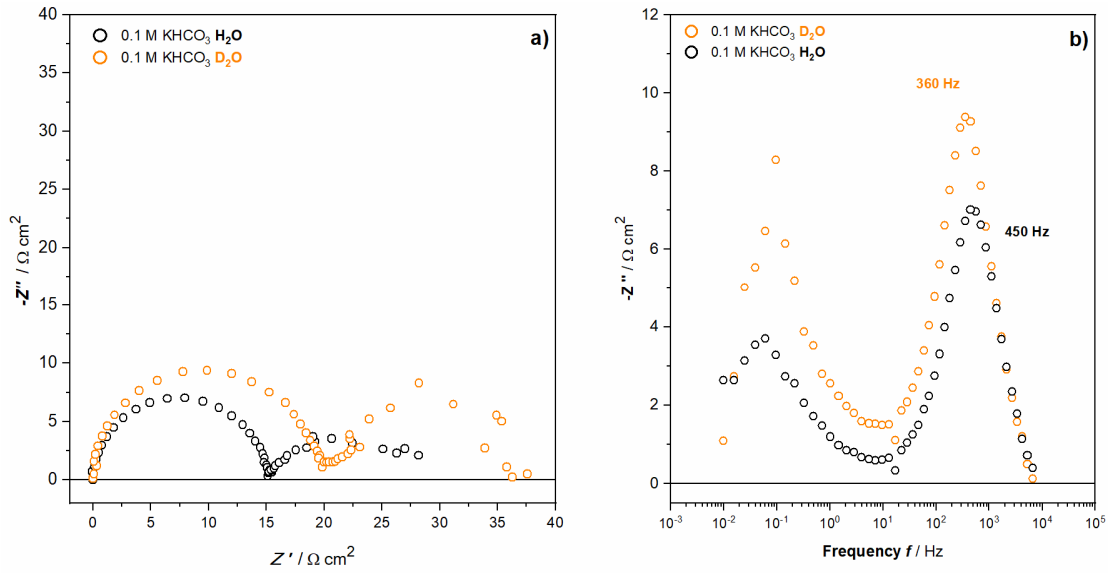


**Figure 3 a)** Impedance spectra and **b)** imaginary part vs. frequency plot for tin foil obtained in $CO_2$ saturated 0.1 M $KHCO_3$ solution comparing $H_2O$ and $D_2O$ as solvent. Galvanostatic operation at – 4.77 mA $cm^{-2}$ with an amplitude of 5 mA, ohmic resistance subtracted.

*$KHCO_3$ concentration series in $N_2$ and $CO_2$ saturated electrolyte*

To investigate the influence of the electrolytes concentration impedance measurement were conducted in $N_2$ and $CO_2$ saturated 0.1 M, 0.2 M, 0.5 M and 1.0 M $KHCO_3$ solutions. It can be seen that in $N_2$ saturated electrolyte the high frequency process, the charge transfer, seems to be independent from the $KHCO_3$ concentration while the low frequency process becomes slower at lower $KHCO_3$ concentrations (cf. **Figure 4 a) & b)**). In $N_2$ saturated electrolyte only hydrogen is

detected which means that all displayed features might be linked with the HER. However, a slight increase in the charge transfer resistance with decreasing $KHCO_3$ concentration might be a result of an increasing pH value and slowing down the HER kinetics. The observed deceleration of the low frequency process with decreasing $HCO_3^-$ concentration may be explained by the fact that $HCO_3^-$ can be reduced to hydrogen at the applied potentials as it was shown by Wuttig et al. for Au catalysts and contribute to the total polarization resistance so that the low frequency arc may displays the diffusion of $HCO_3^-$ ions.[34] Recording impedance spectra for $CO_2$ saturated solutions with different $KHCO_3$ concentrations reveals that now both process are accelerated when increasing the $KHCO_3$ concentration as it is shown in **Figure 4 c) & d)**. The increased charge transfer resistance can be explained taking Eq (1) and **Figure 1b**) into account: The Tafel slope (calculated with total current) increases with reduced $KHCO_3$ concentrations and consequently resulting in higher $R_{Ct}$ values. As it was shown above the $R_{Ct}$ values of the $KHCO_3$ concentration series in $N_2$ saturated electrolytes remain more or less constant which was also observed in the LSV evaluation. However, the change of the nearly independent charge transfer in $N_2$ saturated electrolyte regarding the $HCO_3^-$ concentration to a distinct $HCO_3^-$ concentration dependent charge transfer in $CO_2$ saturated electrolyte indicates a contribution of the $CO_2$RR as a reaction itself (higher Tafel slope compared to HER) or a decelerated HER in $CO_2$ saturated electrolyte to the charge transfer arc in the impedance spectrum. The increase of the charge transfer arc in lower concentrated $CO_2$ saturated electrolytes is not a pH effect regarding the HER since this reaction should be favored at more acidic conditions (cf. pH values **Figure 4 c)**).[35] The increasing low frequency arc in low concentrated $CO_2$ saturated electrolytes can also be explained via a possible $HCO_3^-$ diffusion process.

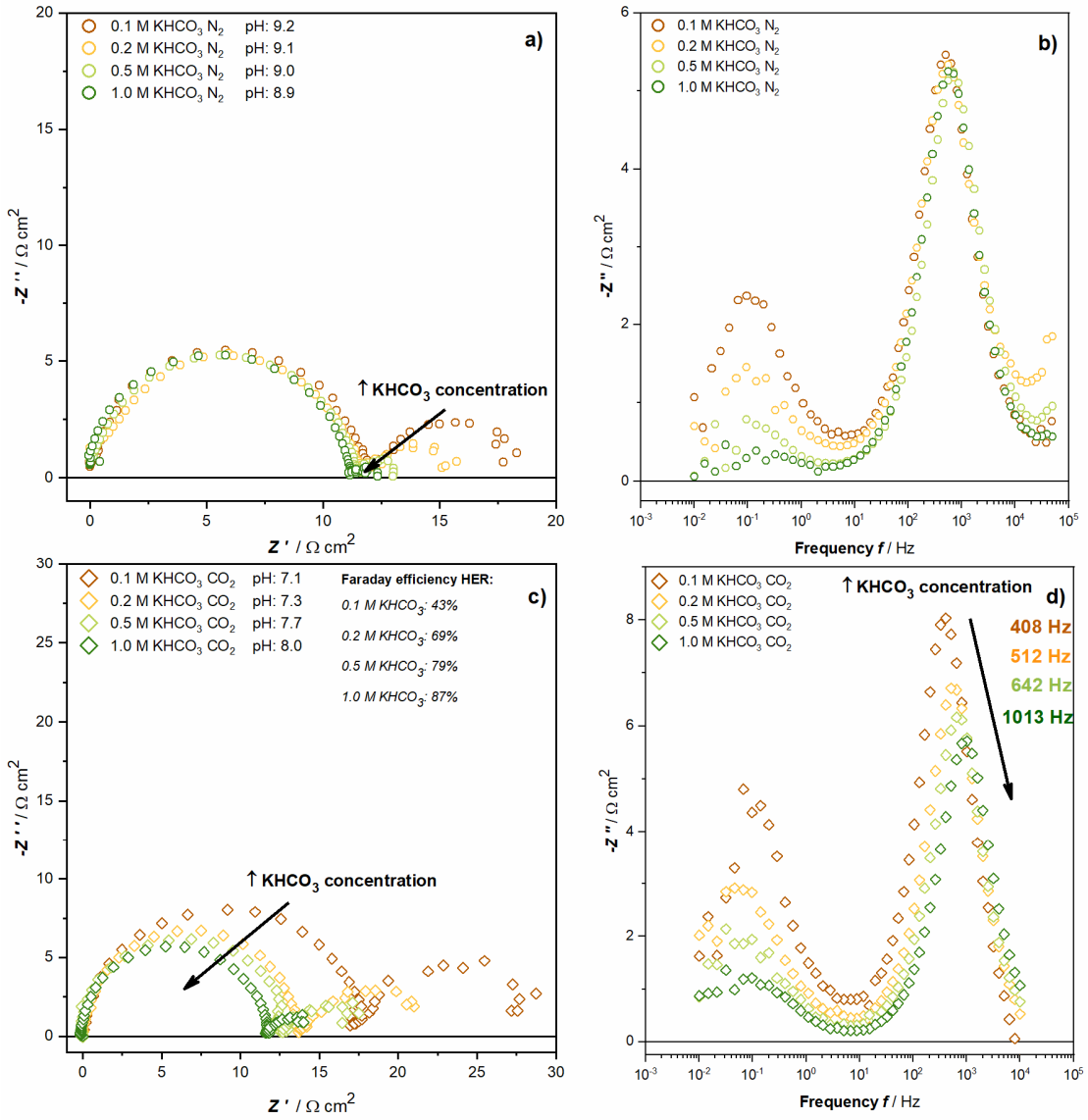


**Figure 4** Impedance spectra obtained for tin foil in aqueous solutions with varying $KHCO_3$ concentrations saturated with **a)** $N_2$ or **c)** $CO_2$ and their corresponding imaginary part vs. frequency plots **b)**, **d)**. Galvanostatic operation at -4.77 mA $cm^{-2}$ with an amplitude of 5 mA, ohmic resistance subtracted.

*Simulating independent parallel occurring charge transfer reactions*

The showed results indicate that the high frequency process displays a charge transfer which is the sum of contributions traced back to the HER and the $CO_2$RR. The reactions occur parallel on the same electrode. **Figure 5 a)** shows an equivalent circuit model (EQCM) simulation for the high frequency process generated with Thales® from ZAHNER-elektrik GmbH & Co. KG assuming one RC element for each reaction (inserted parameters are listed in Table S6). Consequently, the RC elements were combined in parallel since the reactions occur parallel.[36] A parameter study regarding the corresponding time constants $\tau_{HER}$ and $\tau_{CO2RR}$ (regardless which reaction is slowed down) illustrates that for parallel reactions only one arc will be observed in the impedance spectrum no matter how dissimilar the time constants are. When applying the rules of electrical engineering by converting the two resistors and capacitors to one mixed RC element one can see that the simulated –Nyquist plot is identical no matter if the EQCM contains two separate RC elements or one combined RC element (cf. **Figure 5 b)**). This finding supports our theory that the observed charge transfer cannot be exclusively ascribed to the HER or the $CO_2$RR since the parallel occurring reactions will result in one mixed arc during EIS.

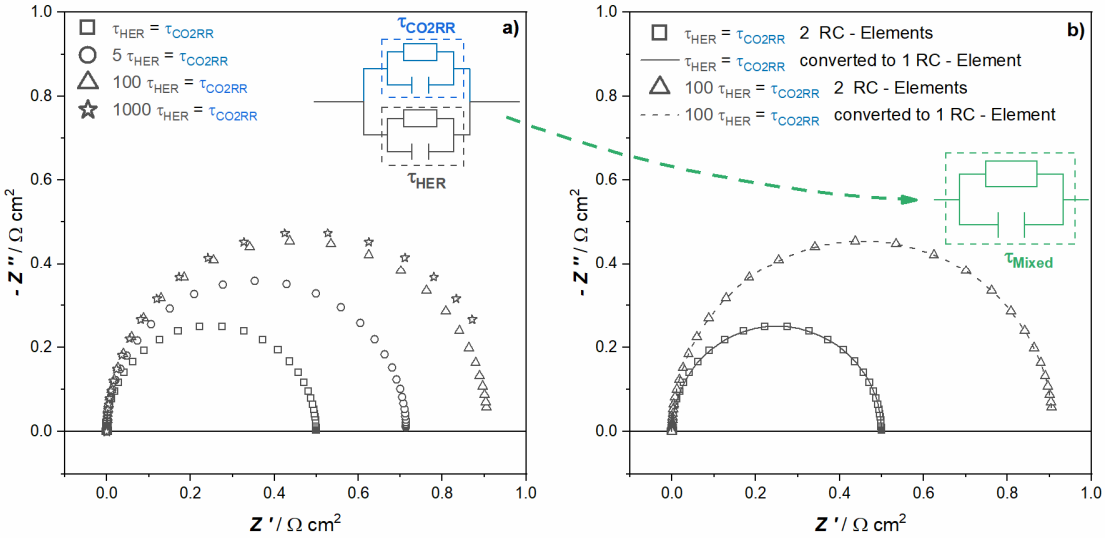


**Figure 5 a)** Simulated EIS spectra for two parallel connected RC elements, representing HER and $CO_2$RR charge transfers on the same electrode surface, with varying time constants showing only one semi-circle no matter how distinct the time constants are **b)** –Nyquist plot of one combined RC element, displaying one mixed time constant for HER and $CO_2$RR, calculated from the parameters of the two RC elements shown in a).

## Conclusion

Impedance spectroscopy reveals at least two observable processes during electrolysis on tin foil in $CO_2$ saturated aqueous $KHCO_3$ solutions. In 1.0 M $KHCO_3$ solution the HER prevailed while in 0.1 M $KHCO_3$ solution $CO_2$RR products dominated the product distribution. A parameter study was carried out to identify the origin of the observed processes for these two cases. Our results indicate that the high frequency process around 500 Hz displays a charge transfer reaction which is determined by the HER and $CO_2$RR no matter if the faraday efficiency for the HER is about 87% (1.0 M $KHCO_3$) or 43% (0.1 M $KHCO_3$). The reactions occur in parallel which we

showed in an EQCM simulation will result in one mixed time constant (RC element) in the EIS spectrum no matter how distinct the difference of the corresponding time constants of the two reactions are. The second process in the low frequency region around 0.1 Hz cannot be reliably identified. Our results suggest that this process may describe the ionic movement in the electrolyte since the resistance of this process scales with the $KHCO_3$ concentration (higher concentration, lower resistance). With our study we wanted to help to identify the observed processes in the EIS spectrum during $CO_2$ electrolysis on tin foil in aqueous $KHCO_3$ solution. Since the HER and $CO_2$RR occur in parallel on the same electrode we showed that the charge transfer resistance measured via EIS is affected by both reactions and cannot easily be used to evaluate catalyst materials. The widely used chronopotentio- or chronoamperometry in combination with the determination of the FEs for $CO_2$RR products are suitable and sufficient methods to evaluate catalysts for $CO_2$RR.

## ASSOCIATED CONTENT

### Supporting Information

The following files are available free of charge.

Determination of faraday efficiencies on tin foil for galvanostatic electrolysis in $CO_2$ saturated 1.0 M $KHCO_3$ solution. EIS spectra for tin foil depending on temperature, applied current and solvent ($H_2O$ vs. $D_2O$) for $CO_2$ saturated 0.1 M and 1.0 M $KHCO_3$ solutions. (PDF)

### Corresponding Authors

*Fabian Bienen, E-mail: Fabian.Bienen@dlr.de

*K. Andreas Friedrich, E-mail: Andreas.Friedrich@dlr.de

### ORCID

Fabian Bienen: https://orcid.org/0000-0002-4660-8826

K. Andreas Friedrich: https://orcid.org/0000-0002-2968-5029

### Author Contributions

The manuscript was written through contributions of all authors. All authors have given approval to the final version of the manuscript.

### Notes

The authors declare no competing financial interest.

## ACKNOWLEDGMENT

Parts of this work were funded by the Federal Ministry for Economic Affairs and Energy (FKZ 03ET1379A/B –EnElMi2.0).

1. Abanades, J. C.; Rubin, E. S.; Mazzotti, M.; Herzog, H. J., On the climate change mitigation potential of CO2 conversion to fuels. *Energy & Environmental Science* 2017, *10* (12), 2491-2499, *DOI 10.1039/C7EE02819A*
2. Smith, P.; Davis, S. J.; Creutzig, F.; Fuss, S.; Minx, J.; Gabrielle, B.; Kato, E.; Jackson, R. B.; Cowie, A.; Kriegler, E.; van Vuuren, D. P.; Rogelj, J.; Ciais, P.; Milne, J.; Canadell, J. G.; McCollum, D.; Peters, G.; Andrew, R.; Krey, V.; Shrestha, G.; Friedlingstein, P.; Gasser, T.; Grübler, A.; Heidug, W. K.; Jonas, M.; Jones, C. D.; Kraxner, F.; Littleton, E.; Lowe, J.; Moreira, J. R.; Nakicenovic, N.; Obersteiner, M.; Patwardhan, A.; Rogner, M.; Rubin, E.; Sharifi, A.; Torvanger, A.; Yamagata, Y.; Edmonds, J.; Yongsung, C., Biophysical and economic limits to negative CO2 emissions. *Nature Climate Change* 2015, *6* (1), 42-50, *DOI 10.1038/nclimate2870*
3. Jouny, M.; Luc, W.; Jiao, F., General Techno-Economic Analysis of CO2 Electrolysis Systems. *Industrial & Engineering Chemistry Research* 2018, *57* (6), 2165-2177, *DOI 10.1021/acs.iecr.7b03514*
4. Zhang, W.; Hu, Y.; Ma, L.; Zhu, G.; Wang, Y.; Xue, X.; Chen, R.; Yang, S.; Jin, Z., Progress and Perspective of Electrocatalytic CO2 Reduction for Renewable Carbonaceous Fuels and Chemicals. *Advanced Science* 2017, *5* (1), 1700275, *DOI 10.1002/advs.201700275*
5. Kortlever, R.; Shen, J.; Schouten, K. J. P.; Calle-Vallejo, F.; Koper, M. T. M., Catalysts and Reaction Pathways for the Electrochemical Reduction of Carbon Dioxide. *The Journal of Physical Chemistry Letters* 2015, *6* (20), 4073-4082, *DOI 10.1021/acs.jpclett.5b01559*
6. Kibria, M. G.; Edwards, J. P.; Gabardo, C. M.; Dinh, C.-T.; Seifitokaldani, A.; Sinton, D.; Sargent, E. H., Electrochemical CO 2 Reduction into Chemical Feedstocks: From Mechanistic Electrocatalysis Models to System Design. *Advanced Materials* 2019, 1807166, *DOI 10.1002/adma.201807166*
7. Scibioh, M. A.; Viswanathan, B., Electrochemical Reduction of CO 2. In *Carbon Dioxide to Chemicals and Fuels*, Elsevier 2018; 307-371, *DOI 10.1016/B978-0-444-63996-7.00007-9*
8. Birdja, Y. Y.; Pérez-Gallent, E.; Figueiredo, M. C.; Göttle, A. J.; Calle-Vallejo, F.; Koper, M. T. M., Advances and challenges in understanding the electrocatalytic conversion of carbon dioxide to fuels. *Nature Energy* 2019, 732-745, *DOI 10.1038/s41560-019-0450-y*
9. Bienen, F.; Kopljar, D.; Löwe, A.; Assmann, P.; Stoll, M.; Rössner, P.; Wagner, N.; Friedrich, A.; Klemm, E., Utilizing Formate as an Energy Carrier by Coupling CO 2 Electrolysis with Fuel Cell Devices. *Chemie Ingenieur Technik* 2019, 872-882, *DOI 10.1002/cite.201800212*
10. Hietala, J.; Vuori, A.; Johnsson, P.; Pollari, I.; Reutemann, W.; Kieczka, H., Formic Acid. In *Ullmann's Encyclopedia of Industrial Chemistry*, John Wiley and Sons 2016; 1-22, *DOI 10.1002/14356007.a12_013.pub3*
11. Verma, S.; Kim, B.; Jhong, H.-R. M.; Ma, S.; Kenis, P. J. A., A Gross-Margin Model for Defining Technoeconomic Benchmarks in the Electroreduction of CO2. *ChemSusChem* 2016, *9* (15), 1972-1979, *DOI 10.1002/cssc.201600394*
12. Agarwal, A. S.; Zhai, Y.; Hill, D.; Sridhar, N., The Electrochemical Reduction of Carbon Dioxide to Formate/Formic Acid: Engineering and Economic Feasibility. *ChemSusChem* 2011, *4* (9), 1301-1310, *DOI 10.1002/cssc.201100220*
13. Raistrick, I. D.; Macdonald, J. R.; Franceschetti, D. R., *Impedance Spectroscopy: Theory, Experiment, and Applications, Third Edition*. John Wiley and Sons 2018; p 21-105, *DOI 10.1002/9781119381860.ch2*

14. Sacco, A., Electrochemical impedance spectroscopy as a tool to investigate the electroreduction of carbon dioxide: A short review. *Journal of CO2 Utilization* 2018, *27*, 22-31, *DOI 10.1016/j.jcou.2018.06.020*
15. Choi, S. Y.; Jeong, S. K.; Kim, H. J.; Baek, I.-H.; Park, K. T., Electrochemical Reduction of Carbon Dioxide to Formate on Tin–Lead Alloys. *ACS Sustainable Chemistry & Engineering* 2016, *4* (3), 1311-1318, *DOI 10.1021/acssuschemeng.5b01336*
16. Lv, W.; Zhou, J.; Kong, F.; Fang, H.; Wang, W., Porous tin-based film deposited on copper foil for electrochemical reduction of carbon dioxide to formate. *International Journal of Hydrogen Energy* 2016, *41* (3), 1585 - 1591, *DOI 10.1016/j.ijhydene.2015.11.100*
17. Daiyan, R.; Lu, X.; Saputera, W. H.; Ng, Y. H.; Amal, R., Highly Selective Reduction of CO2 to Formate at Low Overpotentials Achieved by a Mesoporous Tin Oxide Electrocatalyst. *ACS Sustainable Chemistry & Engineering* 2018, *6* (2), 1670-1679, *DOI 10.1021/acssuschemeng.7b02913*
18. Zeng, J.; Bejtka, K.; Ju, W.; Castellino, M.; Chiodoni, A.; Sacco, A.; Farkhondehfal, M. A.; Hernandez, S.; Rentsch, D.; Battaglia, C.; Pirri, C. F., Advanced Cu-Sn foam for selectively converting CO 2 to CO in aqueous solution. *Applied Catalysis B: Environmental* 2018, *236*, 475-482, *DOI 10.1016/j.apcatb.2018.05.056*
19. Qiao, J.; Liu, Y.; Zhang, J., *Electrochemical Reduction of Carbon Dioxide: Fundamentals and Technologies*. CRC Press 2016, *DOI 10.1201/b20177*
20. Azuma, M.; Hashimoto, K.; Hiramoto, M.; Watanabe, M.; Sakata, T., Electrochemical Reduction of Carbon Dioxide on Various Metal Electrodes in Low-Temperature Aqueous KHCO 3 Media. *Journal of The Electrochemical Society* 1990, *137* (6), 1772-1778, *DOI 10.1149/1.2086796*
21. Narayanan, S. R.; Haines, B.; Soler, J.; Valdez, T. I., Electrochemical Conversion of Carbon Dioxide to Formate in Alkaline Polymer Electrolyte Membrane Cells. *Journal of The Electrochemical Society* 2011, *158* (2), A167-A173, *DOI 10.1149/1.3526312*
22. Reier, T.; Oezaslan, M.; Strasser, P., Electrocatalytic Oxygen Evolution Reaction (OER) on Ru, Ir, and Pt Catalysts: A Comparative Study of Nanoparticles and Bulk Materials. *ACS Catalysis* 2012, *2* (8), 1765-1772, *DOI 10.1021/cs3003098*
23. Lasia, A., Hydrogen evolution reaction. In *Handbook of Fuel Cells*, John Wiley and Sons 2010; 416-440, *DOI 10.1002/9780470974001.f204033*
24. Chen, Y.; Kanan, M. W., Tin Oxide Dependence of the CO2 Reduction Efficiency on Tin Electrodes and Enhanced Activity for Tin/Tin Oxide Thin-Film Catalysts. *Journal of the American Chemical Society* 2012, *134* (4), 1986-1989, *DOI 10.1021/ja2108799*
25. Zhang, Y.; Chen, L.; Li, F.; Easton, C. D.; Li, J.; Bond, A. M.; Zhang, J., Direct Detection of Electron Transfer Reactions Underpinning the Tin-Catalyzed Electrochemical Reduction of CO2 using Fourier-Transformed ac Voltammetry. *ACS Catalysis* 2017, *7* (7), 4846-4853, *DOI 10.1021/acscatal.7b01305*
26. Orazem, M. E.; Tribollet, B., Model-Based Graphical Methods. In *Electrochemical Impedance Spectroscopy*, John Wiley and Sons 2008; 353-362, *DOI 10.1002/9780470381588.ch18*
27. Orazem, M. E.; Tribollet, B., Kinetic Models. In *Electrochemical Impedance Spectroscopy*, John Wiley and Sons 2008; 163-181, *DOI 10.1002/9780470381588.ch10*
28. Chen, Y.; Li, C. W.; Kanan, M. W., Aqueous CO2 reduction at very low overpotential on oxide-derived Au nanoparticles. *J Am Chem Soc* 2012, *134* (49), 19969-19972, *DOI 10.1021/ja309317u*

29. Chen, Z.; Fan, T.; Zhang, Y.-Q.; Xiao, J.; Gao, M.; Duan, N.; Zhang, J.; Li, J.; Liu, Q.; Yi, X.; Luo, J.-L., Wavy SnO2 catalyzed simultaneous reinforcement of carbon dioxide adsorption and activation towards electrochemical conversion of CO2 to HCOOH. *Applied Catalysis B: Environmental* 2020, *261*, *DOI 10.1016/j.apcatb.2019.118243*
30. Wuttig, A.; Yoon, Y.; Ryu, J.; Surendranath, Y., Bicarbonate Is Not a General Acid in Au-Catalyzed CO2 Electroreduction. *Journal of the American Chemical Society* 2017, *139* (47), 17109-17113, *DOI 10.1021/jacs.7b08345*
31. Lee, J. H.; Tackett, B. M.; Xie, Z.; Hwang, S.; Chen, J. G., Isotopic Effect on Electrochemical CO2 Reduction Activity and Selectivity in H2O- and D2O-based Electrolytes over Palladium. *Chemical Communications* 2019, 56, 106-108, *DOI 10.1039/c9cc07611e*
32. Pocker, Y.; Bjorkquist, D. W., Stopped-flow studies of carbon dioxide hydration and bicarbonate dehydration in water and water-d2. Acid-base and metal ion catalysis. *Journal of the American Chemical Society* 1977, *99* (20), 6537-6543, *DOI 10.1021/ja00462a012*
33. Baruch, M. F.; Pander, J. E.; White, J. L.; Bocarsly, A. B., Mechanistic Insights into the Reduction of CO2 on Tin Electrodes using in Situ ATR-IR Spectroscopy. *ACS Catalysis* 2015, *5* (5), 3148-3156, *DOI 10.1021/acscatal.5b00402*
34. Wuttig, A.; Yaguchi, M.; Motobayashi, K.; Osawa, M.; Surendranath, Y., Inhibited proton transfer enhances Au-catalyzed CO2-to-fuels selectivity. *Proceedings of the National Academy of Sciences* 2016, *113* (32), E4585-E4593, *DOI 10.1073/pnas.1602984113*
35. Dubouis, N.; Grimaud, A., The hydrogen evolution reaction: from material to interfacial descriptors. *Chemical Science* 2019, *10* (40), 9165-9181, *DOI 10.1039/c9sc03831k*
36. Sluyters-Rehbach, M., Impedances of electrochemical systems: Terminology, nomenclature and representation - Part I: Cells with metal electrodes and liquid solutions (IUPAC Recommendations 1994). *Pure and Applied Chemistry* 1994, *66* (9), 1831-1891, *DOI 10.1351/pac199466091831*

**SYNOPSIS**

$CO_2$ electrolysis utilizes $CO_2$ as feedstock; we employed electrochemical impedance spectroscopy to understand the microscopic processes at the $CO_2$ converting electrode.

**TOC /Abstract Graphic**

For Table of Contents Use Only.